Structures 2 (2015) 81–90

Contents lists available at ScienceDirect

Structures

journal homepage: http://www.elsevier.com/locate/structures

Effective width equations accounting for element interaction for cold-formed stainless steel square and rectangular hollow sections

M. Bock *, E. Real

Department of Construction Engineering, Universitat Politècnica de Catalunya, UPC, C/ Jordi Girona, 1-3.08034 Barcelona, Spain

ARTICLE INFO

Article history:
Received 9 November 2014
Received in revised form 11 February 2015
Accepted 18 February 2015
Available online 28 February 2015

Keywords:
Cold-formed
Effective width equation
Element interaction
Numerical modelling
Local buckling
Slender cross-sections
Slenderness limits
Stainless steel

ABSTRACT

Rectangular hollow sections featuring high height-to-width (aspect) ratios have shown to offer improved ultimate capacity due to the effects of the interaction between the elements within the cross-section which are particularly significant for slender cross-sections (Class 4) undergoing local buckling. The European design rules dealing with stainless steel, EN 1993-1-4 [1], utilises the concept of cross-section classification and the effective width method for the design of slender cross-sections susceptible to local buckling neglecting such interaction effects, hence resulting in conservative predictions. This paper examines the benefits of element interaction effects on cold-formed ferritic stainless steel compressed sections on the basis of carefully validated finite element models. Following parametric studies, the applicability of various alternative design approaches accounting for element interaction to ferritic stainless steel is assessed and effective width curves, as well as a Class 3 limiting slenderness equation, are derived herein as an explicit function of the aspect ratio. Comparisons with the loads achieved in the FE models have shown that the proposed effective width equations allowing for the benefits of element interaction improve capacity predictions making design more cost-effective.

1. Introduction

The increased material price of stainless steel has always discouraged its use in the construction industry. However, stainless steel's favourable properties may result in decreased expenditure through its life provided they are designed efficiently [2]. Thereby, a better understanding of their structural behaviour is essential to use stainless steel more wisely. Structural research programmes conducted across the world have caused a significant impact on usage of stainless steel in construction and design guidance development [3]. Notable experimental studies concerning local buckling response of hollow sections include [4–6] covering austenitic stainless steel and [7,8] on high-strength stainless steel (high-strength austenitic and duplex stainless steel) among others. The nickel content of these grades, however, particularly affects their costs which led to the investigation of more price-stable alternatives such as lean duplex grades [9] and ferritic grades [10]. The structural applications of this latter type of stainless steel have been recently investigated within a European Project framework and comprehensive design guidance for construction applications has been developed [11]. For the local buckling proposed design provisions, which were firstly based on numerical analyses [12,13], experimental research [14] was undertaken to provide further verification and is presented hereafter.

The purpose of this paper is to investigate the element interaction effects on cold-formed ferritic stainless steel sections comprising slender elements in compression. The sections taken into account were square and rectangular hollow sections (SHS and RHS, respectively). Owing to the cross-sectional shape of the former and when subjected to uniform compression, the four constituent plate elements are equally restrained to one another and simply supported conditions can be assumed at the interconnected boundaries between these plates. However, in a uniformly compressed RHS, the two short plate elements provide additional edge restraints to the longer elements and the boundary conditions tend towards fixed supports as the aspect ratio increases. These element interaction effects result in improved compression capacity and are particularly significant in RHS comprising slender elements. The benefits of such additional restraints are examined herein numerically by using the finite element model (FE) package ABAQUS. The results were used to assess the suitability and performance of various design methods that were developed or used for carbon steel and/or other stainless steel to ferritic stainless steel. These include the classic effective width method and Class 3 slenderness limit given in EN 1993-1-4 [1] and those revised by Gardner and Theofanous [15], which neglect such interaction effects, as well as alternative design approaches that account for element interaction. For these latter methods, the Direct Strength Method (DSM) [16] developed by Schafer and adapted for stainless steel by Becque et al. [17], the regression analysis method proposed by Kato [18] and modified by Theofanous and Gardner [19], and the effective cross-

* Corresponding author. Tel.: +34 934054156; fax: +34 934054135.
E-mail address: marina.bock@upc.edu (M. Bock).

http://dx.doi.org/10.1016/j.istruc.2015.02.003
2352-0124/

section method proposed by Zhou et al. [20] were considered. One additional design approach worthy of mention, but not detailed here further as its potential is exploited for more complex cross-sections than those considered herein, is the Generalised Beam Theory (GBT) pioneered by Schardt in Germany [21], extended by Davies in Britain [22,23] and actively upgraded over the last years by Camotim and his colleagues in Portugal [24,25].

Finally, a modification is proposed so that the effective width method accounts for the benefits of element interaction by inserting the aspect ratio within both the reduction factor ρ equation and the Class 3 limiting slenderness value. The proposed amendment is statistically validated following the guidelines given in Annex D of EN 1990 [26] and compared with existing test results to verify its applicability to all stainless steel families.

2. Numerical investigation

2.1. Modelled stub column tests

In order to numerically investigate the benefits of element interaction effects on ferritic stainless steel slender sections, and because of the limited available experimental data on the performance of this type of cross-sections, only the experimental investigation conducted by the authors on cold-formed ferritic stainless steel slender sections [14] is considered herein to develop and validate a comprehensive FE model using the FE package ABAQUS. Bock et al. [14] reported the results of 8 stub column tests performed on 4 different SHS and RHS (two repeated tests on each cross-section), including the measurements of such geometries and initial local imperfections w_0, as given in Table 1 where L is the length of the specimen, H is the overall height, B is the overall width, t is the thickness, r_i is the internal corner radius, α is the aspect ratio and A is the gross cross-sectional area (see Fig. 1). Note that these tests were particularly suitable to validate the FE model owing to the various aspect ratios of the specimens.

Material properties were derived from coupon tests in [14], including tensile flat and corner coupons. The formers were extracted from flat faces of the specimens whereas the latter were taken from the curved portions of each of the cross-sections to quantify the corner strength enhancements induced by the cold-forming process [27].

Experimental observations in the corner regions [28] concluded that this enhanced strength extends into the flat regions by a distance equal to two times the material thickness. This remark has been used in previous numerical studies on other stainless steel grades [29,30] and adopted herein. Measurements of residual stresses were not explicitly taken in [14] since they are inherently present (i.e., through-thickness residual stresses) in material properties extracted from cold-formed sections [4] and have shown little influence on the cross-sectional response [31]. The material properties determined in [14] are summarized in Table 2 for the four sections where the reported parameters are the Young's modulus E, the 0.01%, 0.05% and 0.2% proof stress $\sigma_{0.01}$, $\sigma_{0.05}$ and $\sigma_{0.2}$, respectively, and the ultimate stress σ_u with its corresponding ultimate strain ε_u. Table 3 gives the weighted average values based on face width and corner properties extended two times the thickness through the flat region for all the tested specimens while Table 4 shows the average material properties of all the flat and corner tensile coupon tests. These sets of material properties are used in the following sections to assess their influence on the numerical response.

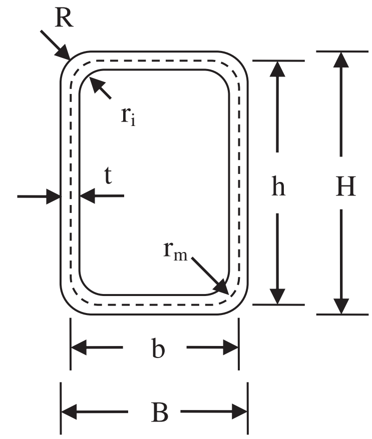

Fig. 1. Definition of symbols.

All the specimens were uniformly compressed between flat platens in an Instron 1000 kN hydraulic testing machine which was driven by displacement control. The achieved test load $N_{u,test}$ and its corresponding specimen's end shortening δ_u are given in Table 1.

2.2. Finite element model

The FE analysis package ABAQUS was used to simulate the cross-sectional response of the 8 ferritic stainless steel compression SHS and RHS tested in [14]. The measured geometric properties given in Table 1 were used in the FE model, which was based on the centreline dimensions of the cross-sections h × b × r_m (see Fig. 1). The geometry of all the specimens was discretized using the four-node general-purpose shell element with reduced integration S4R [32,33], including both flat parts and curved regions of the cross-sections. The geometry of these latter regions was approximated by 3 linear elements. The flat regions adjacent on either side of the corners, which are affected by the cold-forming process exhibiting enhanced strength, were discretized using two elements, each of them with size equal to the thickness of the cross-section. For the remainder flat portion, mesh studies were conducted to achieve accurate results while minimizing computational time obtaining a suitable mesh size of 8 × 8 mm.

Owing to the double symmetry of the geometry, boundary conditions, applied loads and observed failure modes in the experimental investigation [14], only a quarter of the section with suitable

Table 1
Measured dimensions and test results [14].

Specimen	L (mm)	H (mm)	B (mm)	t (mm)	R (mm)	r_i (mm)	A (mm^2)	α	w_0 (mm)	$N_{u,tests}$ (kN)	δ_u (mm)
60 × 60 × 2-SC1	179.5	60.3	60.3	2.00	4.4	2.4	454	1	0.02	211.37	1.02
60 × 60 × 2-SC2	180.0	60.3	60.4	2.02	4.4	2.3	460	1	0.02	212.31	1.03
70 × 50 × 2-SC1	210.0	70.1	49.9	2.00	4.3	2.3	451	1.4	0.03	190.15	0.87
70 × 50 × 2-SC2	210.0	70.0	49.8	1.99	4.2	2.2	450	1.4	0.03	190.05	0.84
80 × 40 × 2-SC1	240.0	80.0	40.5	2.00	3.3	1.3	457	2	0.06	178.21	0.80
80 × 40 × 2-SC2	240.0	80.0	40.3	1.99	3.9	1.9	453	2	0.06	179.52	0.82
100 × 40 × 2-SC1	299.5	100.1	40.0	2.05	4.1	2.1	546	2.5	0.07	184.23	0.97
100 × 40 × 2-SC2	299.5	100.1	40.5	1.99	4.2	2.2	532	2.5	0.07	183.99	0.92